Talanta 103 (2013) 236–244

Contents lists available at SciVerse ScienceDirect

Talanta

journal homepage: www.elsevier.com/locate/talanta

# Feasibility of digital image colorimetry—Application for water calcium hardness determination

Angel Lopez-Molinero*, Valle Tejedor Cubero, Rosa Domingo Irigoyen, Daniel Sipiera Piazuelo

*Department of Analytical Chemistry, Faculty of Sciences, University of Zaragoza, 50009 Zaragoza, Spain*

ARTICLE INFO

*Article history:*
Received 10 August 2012
Received in revised form
8 October 2012
Accepted 11 October 2012
Available online 3 November 2012

*Keywords:*
Digital image colorimetry
RGB color
PCA
Fourier transform
Water calcium hardness determination.

ABSTRACT

Interpretation and relevance of basic RGB colors in Digital Image-Based Colorimetry have been treated in this paper. The studies were carried out using the chromogenic model formed by the reaction between Ca(II) ions and glyoxal bis(2-hydroxyanil). It produced orange–red colored solutions in alkaline media. Individual basic color data (RGB) and also the total intensity of colors, $I_{tot}$, were the original variables treated by Factorial Analysis. Te evaluation evidenced that the highest variance of the system and the highest analytical sensitivity were associated to the G color. However, after the study by Fourier transform the basic R color was recognized as an important feature in the information. It was manifested as an intrinsic characteristic that appeared differentiated in terms of low frequency in Fourier transform. The Principal Components Analysis study showed that the variance of the system could be mostly retained in the first principal component, but was dependent on all basic colors.

The colored complex was also applied and validated as a Digital Image Colorimetric method for the determination of Ca(II) ions. RGB intensities were linearly correlated with Ca(II) in the range 0.2–2.0 mg $L^{-1}$. In the best conditions, using green color, a simple and reliable method for Ca determination could be developed. Its detection limit was established (criterion 3 s) as 0.07 mg $L^{-1}$. And the reproducibility was lower than 6%, for 1.0 mg $L^{-1}$ Ca. Other chromatic parameters were evaluated as dependent calibration variables. Their representativeness, variance and sensitivity were discussed in order to select the best analytical variable.

The potentiality of the procedure as a field and ready-to-use method, susceptible to be applied 'in situ' with a minimum of experimental needs, was probed. Applications of the analysis of Ca in different real water samples were carried out. Water of the city net, mineral bottled, and natural-river were analyzed and results were compared and evaluated statistically. The validity was assessed by the alternative techniques of flame atomic absorption spectroscopy and titrimetry. Differences were appreciated but they were consistent with the applied methods.

## 1. Introduction

Calcium is a common content in natural waters and constitutes, together with magnesium, the major components of water hardness. In drinking water it is considered a natural and mineral nutrient. World Health Organization (WHO) has published a monograph on public health significance of water hardness [1] in which its benefits and risks are discussed.

Guides for the quality of drinking water of WHO have not established value limits for the content of Ca regarding its health acceptability. Neither have UE and USA legislations. Notwithstanding, a taste threshold has been signaled in the range of 100–300 mg $L^{-1}$ with a maximum tolerance up to contents at level of 500 mg $L^{-1}$ [2].

According to previous reports, the need for control and surveillance of the Ca content in water is strongly related to the water use. It is a well known and documented fact that high Ca content hard waters could give rise to $CaCO_3$ deposits, while low Ca content, 100 mg/l, soft waters could decrease the buffering capacity and favor the corrosion of water pipes. Consequently the determination of water hardness in general, and Ca as its basic component, is profusely carried out in many laboratories as part of its sustainable transport and storage.

Routine determinations of Ca could be realized by different analytical methods. Standardized procedures based on international standards are applied worldwide. A classic complexometric titration is the basis for the ISO 6058 [3]. It is a standard that could be directly applied for Ca determination in water with contents in the range 2–100 mg/l. The Gravimetric determination

---

* Corresponding author. Fax: +34 976 761 292.
*E-mail address:* anlopez@unizar.es (A. Lopez-Molinero).

0039-9140/$ - see front matter © 2012 Elsevier B.V. All rights reserved.
http://dx.doi.org/10.1016/j.talanta.2012.10.038

by oxalate precipitation establishes another reference method which could easily be implemented by permanganate titration of the calcium oxalate precipitate.

Atomic spectrometric methods are well adapted to perform this determination. Flame Atomic Absorption Spectrophotometry (FAAS) [4] is a very selective and sensitive method. Typical LD values are in the order of 0.1 mg $L^{-1}$, with linear range up to 5 mg/l, using standard acetylene–air flame conditions. However, interferences due to ionization, stable oxysalt production and bicarbonate formation should be taken into account to produce accuracy results. More sensitive techniques, such as ICP-OES [5], with 0.19 μg $L^{-1}$ LD at 393.366 nm, are available.

Molecular spectrometric techniques represent a common alternative. Many of them are suited to trace analysis and require adaptation steps for real sample analysis that, consequently, contribute to the uncertainty increase in final results. Molecular Absorption Spectrophotometry allows the UV–vis determination of Ca and Mg after developing colored complexes with metallochromic reagents. Simple and automatic determination by Eriochrome Black T (EBT), with concentration ranges in the order of 3–40 mg $L^{-1}$, was promptly established [6]. Multiple determinations in water, besides hardness, based on modern Diode arrays technology with PLS calibration and pyridylazo resorcinol as reagent, have also been implemented [7]. Recently, screening and tentative fast methods have been developed. They are based on flow injection systems (FIA) with UV–vis detection using EBT as indicator [8], or by light scattering [9]. Also potentiometric detection has been used. This last was based on solid composite electrodes with quinhydrone [10]. The method presented LD's in the range of 0.4 mg $L^{-1}$for Ca and Mg. A high selectivity has been recently described by Molecular Fluorescence with the use of aptamers [11]. This method was based on labeled olygonucleotides acting as fluorescent reagent. LDs were in the order of 1.6 mg $L^{-1}$with linear ranges up to 20 mg $L^{-1}$, for Ca and Mg.

Procedures with special current analytical interest are those defined as ready-to-use and field methods. They are suitable for rapid surveillance in fields with high demand of analysis such as clinical or environmental and could be applied in quantitative and semi-quantitative determinations. The strategic paper of these types of methods has been recognized by the most important chemical manufacturers [12]. ISO has recognized the importance of the ready-to use methods, in particular in environmental-water analysis, and has issued an important guide [13].

Digital Image-based methods [14], in particular Digital Image Colorimetry (DIC) [15] could be considered as a new type of ready method. It uses easily captured digital images with accessible digital cameras, web-cams or hand scanners. They are equipped with Complementary Metal-Oxide Semiconductors (CMOS) or Charge Coupled Detectors (CCD) that could provide fast Red Green Blue basic colors of chromogenic processes-systems.

Two principal possibilities could be recognized in DIC. On one hand, reactions and processes based on intrinsic colors, that is, when the same reagents or products are used experiment a color change. Such is the case of the wine characterization during acidic/basic titration [16]. Or also, by the use of external chromogenic compounds. These react with analytes (as reagents or products) to generate a color change. It is a useful alternative that has allowed to develop fast detection and measurement procedures in many fields for many analytes; for instance, ions and metabolites in biological fluids [17,18], antiseptic type compounds [19], Fe and chlorine in tap water [20], Ti in plastics [15], continuous and automatic monitoring of reagents, in real time, to control industrial electroplating processes [21], semi-quantitative field tests for illicit opiate drug compounds [22], amphetamine and methylamphetamine [23], Ni in iron meteorites [24] or organic pollutants in water [25].

Recently chromoionophore compounds, typically used in optical sensors as immobilized reagents, have been applied as chromogenic selective reagents. Their colored reaction changes could be detected by digital image cameras. In particular they have been applied in water hardness determination [26,27] resulting in best LDs in the order of 65 and 7 μg $L^{-1}$, for Mg and Ca, respectively.

Digital image based-flame emission methods (DIB-FES) represent an alternative to the previous DIC reflected colorimetry. It is based on measurements of colors emitted by a flame. Atomic flame emission methods have been adapted as fast determinations, with the use of web-cam detectors, of easily excited atoms, such as Li, Na and Ca [28]. The method has also been applied for the indirect determination of therapeutic drugs [29].

An interesting point regarding the analytical applicability of digital image-based methods is the selection of the quantitative instrumental variable. In a majority of the published papers, it is based on the intensity, or luminosity, of individual RGB basic colors. In this way, the signal sensitivity is dependent on the sensors depth and, consequently, on the number of bits. So, sensor readings with 8 bits produced responses with sensitivity ranged from 0 to 255 units ($2^8$). And very high sensitivity could be obtained by sensors with 24 bits: 0–16 777 216($2^{24}$). However, others have proposed alternative color-based parameters. They are calculated and derived after addition, product, and logarithm transformation of individual components.

In this work, the analytical feasibility of the basic colors and their representativeness were studied. Also, different chromatic parameters, derived from basic colors, were evaluated as analytical calibration variables. It represents a fundamental work in order to demonstrate the applicability of basic RGB color measurements in analytical determinations. Finally, a method for rapid and quantitative determination of Ca, which relies on color development with a selective reagent, was developed. Results have been applied as a simplified and fast method that could be applied to different samples and validated by comparison with standard reference methods. Its use as a field method has also been probed.

## 2. Material and methods

### 2.1. Apparatus and software

A Perkin-Elmer model 2380 flame atomic absorption spectrometer was used. It was equipped with Perkin-Elmer hollow-cathode lamps. The standard nebulization system was used with burners for air–acetylene (10 cm slot). The atomic absorption (F-AAS) of Ca was measured at 422.7 nm, with 5 mA lamp current, and a blue oxidizing air–$C_2H_2$ flame. Typical dynamic range in solution was maintained: 0–5.0 mg $L^{-1}$ of Ca(II).

Digital compact camera, with the characteristic of Table 1, was used.

MATLAB 6.5 (Mathworks, Natick, MA, USA) for reading colorimetric data (RGB), computing Fast Fourier Transform (fft), Artificial Neural Network- BP algorithm, Principal Components Analysis, PCR regression and also Excel (Microsoft Excel, Redmond, WA,USA) were used.

### 2.2. Reagents

All reagents were of analytical grade and deionized water from a Milli Q water purification system was always used, unless stated otherwise.

Standard Ca(II) solution (500 mg $L^{-1}$) was prepared by dissolving $CaCO_3$ (Panreac, ACS, Barcelona, Spain) with a minimum of

**Table 1**
Characteristic and optimum conditions of the Nikon Coolpix 2100 photographic digital camera for Ca(II) determination.

| | |
|---|---|
| Camera resolution | 2.0 M pixels |
| 'CCD' Sensor | $2.5 \times 6.9$ cm$^2$ (wide/high) |
| Conditions to take pictures | |
| Function 'mode' | Automatic |
| Lighting | Indirect, fluorescent white lamp, 16 wat |
| Focus | 30 cm (without zoom) |
| Exposure | White laboratory-made box |
| Record pictures | 'jpg' format, $1600 \times 1200$ pixels |
| Image processing | |
| Transfer images to the computer | Microsoft photo editor, in Windows XP |
| Color Measurement | Matlab 6.5 |

0.1 M HCl, and dilution with deionized water to the volume of calibrated flasks. Diluted solutions were prepared from the previous concentrated Ca solution by convenient dilution with deionized water in calibrated flasks.

Standard 0.05% (w/v) glyoxal bis(2-hydroxyanil)—GBHA (Sigma-Aldrich, Quimica Madrid, Spain) solution in methanol was prepared.

Eriochrome black T (EBT) (Panreac ACS, Barcelona, Spain) was freshly prepared as 0.1% (w/w) solid dispersion in NaCl.

0.4 M NaOH solution was prepared by dissolving NaOH (Panreac PA, Barcelona, Spain) in deionized water.

0.01 M EDTA solution was prepared by dissolving disodium salt of EDTA ($Na_2$ $H_2C_2O_4.2H_2O$) ( Panreac ACS, Barcelona, Spain) in deionized water and convenient dilution with deionized water to the volume of volumetric flasks. Solution was standardized with Ca(II), at alkaline pH, with Murexide (Panreac ACS, Barcelona, Spain A) as indicator.

### 2.3. Colorimetric procedure

Standard calibration Ca(II) solutions: Five mL of standard GBHA solution, 1 mL of 0.4 M NaOH and 1 mL of diluted standard Ca(II) solution were added to a 10 mL calibrated flask. Then it was diluted to the mark with deionized water.

Water sample solutions were prepared similar to the previous standard calibration solutions but with the addition of 1 mL of sample, instead of the standard Ca(II) solution. Water samples could be directly added, or after appropriate dilution, depending on the Ca(II) content. Natural waters were filtered through 0.49 μm filter in previous determination.

### 2.4. Imaging measurements

Images of calibration and sample solutions, in spectrophotometric cells of 1 cm optical path ($1 \times 1 \times 1.3$ cm$^3$), set all together in a laboratory-made box, were taken using an indirect constant artificial lighting produced by a white cool fluorescent lamp of 18 W. Automatic focus mode, with samples at 30 cm length, was used. The size of the pictures was the smallest size with the camera. Pictures were transferred to a computer using Microsoft Photo Editor (Microsoft XP). Colors were obtained from representative regions of 3000 pixels, approximately, located in each spectrophotometric cell. RGB values were measured, in each pixel, with Matlab's image processing tool box. Afterwards, RGB data of 21 different pixels were averaged. That is, the color in each cell was given by three average data (R,G,B) obtained, each one from 21 individual pixels.

### 2.5. Chromatic variables

Other color-based parameters have been evaluated from the previously measured RGB basic colors. They were calculated according to the models proposed by authors in the bibliography. The following chromatic parameters, CP, were studied [26,28,30]:

$$CPe = 2^R \times 2^G \times 2^B$$

$$CPa = \sqrt{{R_{s-b}}^2 + {G_{s-b}}^2 + {B_{s-b}}^2}$$

$$CPl = \frac{\log(G_s) - \log(G_b)}{\log(G_{max}) - \log(G_b)}$$

with R G B being the luminosity of basic colors experimentally measured.

$R_s$ $G_s$ $B_s$ corresponded to the RGB color of the sample while $R_b$ $G_b$ $B_b$ corresponded to the RGB data of a blank solution (without Ca).

In the same way, $\log(G_s)$, $\log(G_b)$, $\log(G_{max})$ corresponded to the 'log' of the basic G color of sample and blank, while $G_{max}$ corresponded to the G color of the last point of the calibration graph.

## 3. Results and discussion

### 3.1. Chromogenic basis

Ca(II) ions react with GBHA, in 0.04 M NaOH alkaline media, to give an orange–red complex [31]. Beer's law, at 516 nm, was obtained with $1.8 \times 10^4$ L mol$^{-1}$ cm$^{-1}$ M absortivity, with 0.02 mg L$^{-1}$ LD. Linear calibration equation was established $Y = 0.452\ X + 0.0591$. Being $Y$ the absorbance at 516 nm, and $X$ the Ca(II) concentration in mg L$^{-1}$. This procedure does not present interference of Mg(II).

### 3.2. Selection of optimum condition

Conditions to capture images and measure colors in a reproducible way have been previously discussed [15]. The principal factors affecting the measurements, lighting, and focal length were optimized. Exposition and focusing of images were always carried out in a white laboratory-made cabinet, with the automatic function in the camera. Lighting was obtained by using artificial cool white fluorescent of 18 W and cell samples were located at 30 cm from the camera. Other conditions were established in a manner similar to that in the previous published paper.

Different commercial cameras were used, with resolutions ranging from 2 to 7 M pixels. Also a professional camera uEye LE, model UI-1485LE-C (IDS, Imaging Developing Systems, GmbH, Germany) with a resolution of $2560 \times 1920$ pixels, was employed. Results were not affected by the camera type or resolution. Notwithstanding, the results gathered corresponded to the simplest camera of 2 M pixels.

Also, different softwares were applied in the measurements of RGB color data. They included Matlab 6.5, Photoshop CS5 (Adobe), Corel Draw X6 (Corel Corporation) and GIMP 2.0 (GNU Image Manipulation Program). The differences between them were not significant. However, results gathered in the paper were obtained by Matlab 6.5 and using a simplified program developed by us.

### 3.3. Multivariate analysis of color data

Factorial Analysis of color images corresponding to the calibration experience was carried out by Principal Component Analysis (PCA), and taking into consideration four initial variables. They corresponded to the individual RGB color and also to '$I_{tot}$', defined as R+G+B. This last variable, despite its correlation, offered complementary information to the other three and represents the amplitude of the color space and the sensitivity of the detector. The results of the study are gathered in Fig. 1 and Tables 2 and 3.

The covariance–variance matrix corresponding to the initial data-variables showed the variance distribution of the initial color-variables of the system. It could be observed that color G presented the highest variance of colors with more than 50% of the total variance. Red color was the second whereas Blue color presented a low variance. Also, $I_{tot}$ retained an important percentage of the variance. This result demonstrated the significance of the last variable, and consequently an argument for its inclusion as a color variable in order to obtain complete information of the chromogenic system.

The variance values were later compared with the slopes of calibration graphs in analytical calibrations. It could be observed that the percentage of retained variance by each variable was correlated with the slope of the calibration graphs. So the highest variance of the G color corresponded with the highest analytical sensitivity.

The study by Principal Components Analysis (PCA) (with standardized data) demonstrated that the initial colors could be easily reduced and described by new factors. So the main first Principal Component (PC1) accounted for 89% of the initial variance of data. Including the second PC, (PC1+PC2), the accumulated variance attained 97% of the initial data. That is, practically the entire information of the RGB color space could be explained by only two PCs, without significant loss of information.

However, the correlation between the new latent variables, or PCs, and the initial RGB variables demonstrated an equilibrated distribution (without rotation) of the initial basic colors. That is, the loadings between 'Initial Colors' and 'PC1' could be rounded in the order of 0.5. It could be said that the significant PC1 retained information of all the initial variables and had no strong identification with any color.

In a general point of view, the loadings plot, in Fig. 1(b), showed that the basic colors represented different features of information. However R color, identified by its vector, was demonstrated to be very different from the rest of the variables while Green, Blue and also $I_{tot}$ manifested a certain level of similarity.

### 3.4. Colors by Fourier transform (FT)

FT can be used as a data exploratory method. According to it, data are modeled by a series of terms, composed of sine and cosine periodic functions. The significance of each term is determined by the values of the Fourier Coefficients (FCs). These are the amplitude of sine and cosine series. First FCs in a Fourier series are associated to periodic functions of low frequency with significant information while last FCs are associated to high frequencies that, commonly, retain the noise information. Consequently the model decomposes the initial data in different terms and their significance can be evaluated.

This concept was applied to the analytical data in the calibration experiment. That is, calibration data with RGB values were treated by FT and decomposed in serial terms. The pairs of FCs

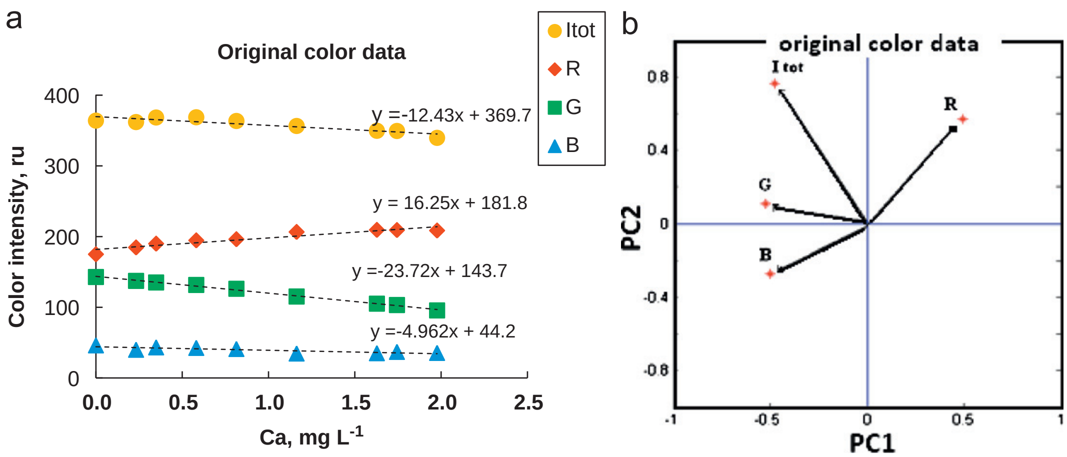

**Fig. 1.** Digital RGB data for orange solutions in a standard Ca(II) calibration graph. Color developed with 0.1 M GBHA at pH 10, buffer $NH_4Cl–NH_3$. (a) Linear calibration with Ca(II) ranging from 0 to 2.0 mg/l; (b) loading plots of color variables over new variables Principal Component 1 and PC2. (For interpretation of the references to color in this figure legend, the reader is referred to the web version of this article.)

**Table 2**
Statistical characteristics of the initial RGB color data and after its reduction by principal component analysis.

| Initial Variable | Retained variance | % Explained variance | % Acumulated variance | | | | |
|---|---|---|---|---|---|---|---|
| R | 152.61 | 27.14 | 27.14 | | | | |
| G | 290.61 | 51.69 | 78.83 | | | | |
| B | 17.11 | 3.04 | 81.87 | | | | |
| Itot | 101.89 | 18.13 | 100.00 | | | | |
| New Component PC | Eigenvalue | % Explained variance | % Acumulated variance | Loadings, initial color variables | | | |
| | | | | R | G | B | Itot |
| 1 | 3.56 | 89.10 | 89.10 | 0.497 | −0.522 | −0.501 | −0.479 |
| 2 | 0.31 | 7.73 | 96.83 | 0.572 | 0.105 | −0.275 | 0.766 |
| 3 | 0.13 | 3.18 | 100.00 | 0.393 | −0.447 | 0.802 | 0.0553 |
| 4 | 0.00 | 0.00 | 100.00 | −0.521 | −0.719 | −0.174 | 0.426 |

were calculated for each standard. Afterwards, the calibration curve was recomposed step by step, that is, by adding consecutive terms of the FT series to re-calculate $RGBI_{tot}$ data.

Figs. 2–4 showed the calibration curves when data colors were sequentially recomposed. In each step, the application of PCA provided a method to interpret the retained information.

It could be seen in Fig. 2(a) that, with the first pair of FCs (really, it is the independent coefficient of the model), a single calibration curve was obtained. All individual colors were superimposed. It was interpreted as a general feature of the system: this information demonstrated a high correlation with Ca concentration but was negative. It could be also argued that this information was associated to the serial term of low frequency and consequently it represented basic and principal information. Fig. 2(b) demonstrated that this information was composed by the individual influence of the R color while the rest of colors offered confounded or indistinguishable information.

The calibration with colors recomposed by including two FCs is gathered in Fig. 3. It was observed that colors could be separated in four components. All of them presented negative slopes. But on one hand, R and $I_{tot}$ were characterized by low slopes while B and G had higher values than the previous colors. The PCA study confirmed these two different behaviors. R and $I_{tot}$ vectors showed similar orientation and consequently expressed coincident information whereas, B and G acted, between them, as similar colors.

The inclusion of the third FCs pair recomposed the colors with the characteristics observed in Fig. 4. It could be seen that now, only G and $I_{tot}$ presented negative slopes and great values, while R and B had positive slopes and low values. The PCA study demonstrated the similarity between the first two colors and the complementary features of the other two colors.

Lately, the original calibration curves could be recomposed by inclusion of the four pairs of data.

The analysis of information by FT demonstrated that as the number of FC pairs was increased, differences appeared between the colors. That is, with the firsts, or low frequency pairs, the common or latent information could be justified. This could be characterized by two principal and different contributions: R color and G color. While the former was interpreted as an intrinsic color feature, the latter was associated with the highest variability of the system, and consequently was the factor most influencing the analytical sensitivity or analytical valuable information.

With the inclusion of the last frequency FC pairs, the magnitude-luminosity of colors increased and differences could be totally confirmed.

The FT study demonstrated the existence of two principal types of information: (a) latent information related to the intrinsic characteristics of the color and linked to the R color, and (b) information related to the variability or analytical sensitivity and which was linked to the G basic color. These participations could be identified in the first terms and were increasingly manifested with the inclusion of the last and high frequency terms.

### 3.5. *Calibration and analytical performance*

The study of images corresponding to a calibration curve shows characteristic trends (see Fig. 1). The apparent luminosity of the orange color increased as the concentration of Ca(II) increased in solutions, while the measured Green color decreased, the Red fairly increased and the Blue color fairly decreased.

These results provided that the highest color sensitivity, vs Ca(II) concentration, was established with the Green color. They were congruent with the study of the variance retained by each color.

Linear calibration graph, under the optimum conditions, could be found between the Green color intensity–luminosity (*Y*, in relative units, ru) and the Ca(II) concentration (*X*, in mg $L^{-1}$),

**Table 3**
Figures of merit of the linear regressions of the complex Ca(II)–GBHA using different chromatic parameters as dependent variable in calibration.

| *Y* Chromatic variable | *X* Variable | Sensitivity, slope | Intercept | Correlation coefficientr | Linear range (mg/l) | Residual Standard Deviation |
|---|---|---|---|---|---|---|
| G, ru | Ca, mg/l | −23.63 | 144.0 | 0.995 | 0.2–2.0 | 1.85 |
| Log (CPe) | | −5.942 | 12.63 | 0.990 | 0.6–1.7 | 0.55 |
| CPa, ru | | 28.46 | 4.943 | 0.990 | 0.2–2.0 | 3.23 |
| CPl, ru | | 0.633 | −0.204 | 0.999 | 0.6–1.2 | 0.01 |
| Ca, mg/l | PC1 | 0.371 | 0.943 | 0.990 | 0.2–2.0 | |

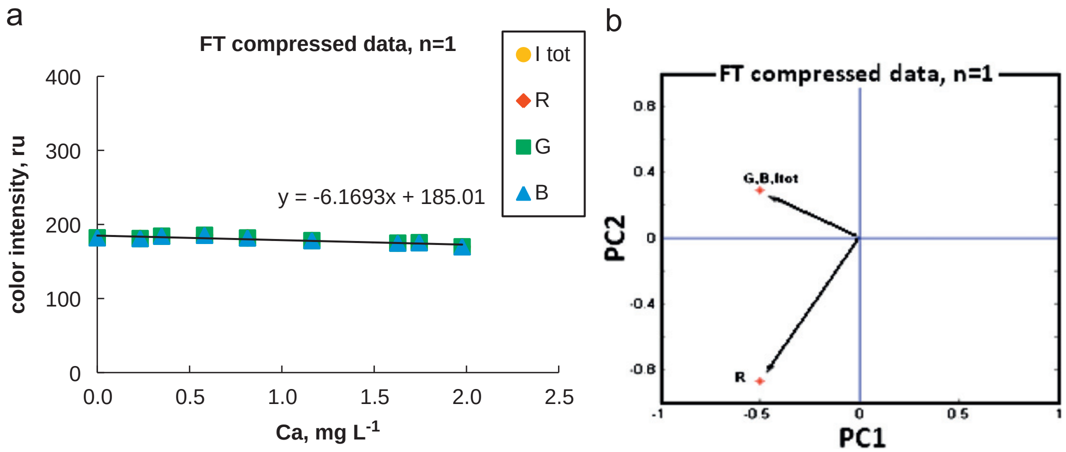

**Fig. 2.** Digital RGB data after compression by FT1, for orange solutions obtained in the standard calibration graph of Fig. 1. (a) Linear calibration using compressed color data; (b) loading plots of color variables over PC1 and PC2. (For interpretation of the references to color in this figure legend, the reader is referred to the web version of this article.)

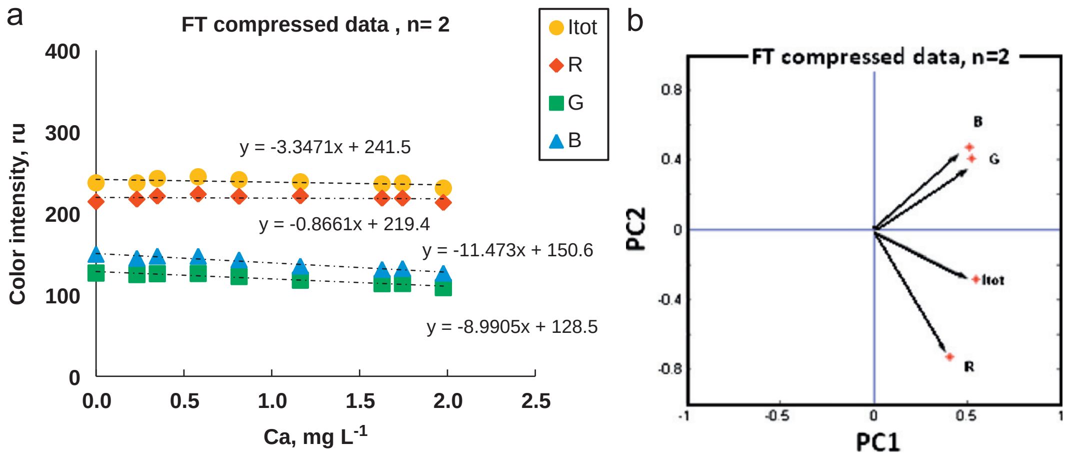

**Fig. 3.** Digital RGB data after compression by FT2, for orange solutions obtained in the standard calibration graph of Fig. 1. (a) Linear calibration using color data; (b) loading plots of color variables over PC1 and PC2. (For interpretation of the references to color in this figure legend, the reader is referred to the web version of this article.)

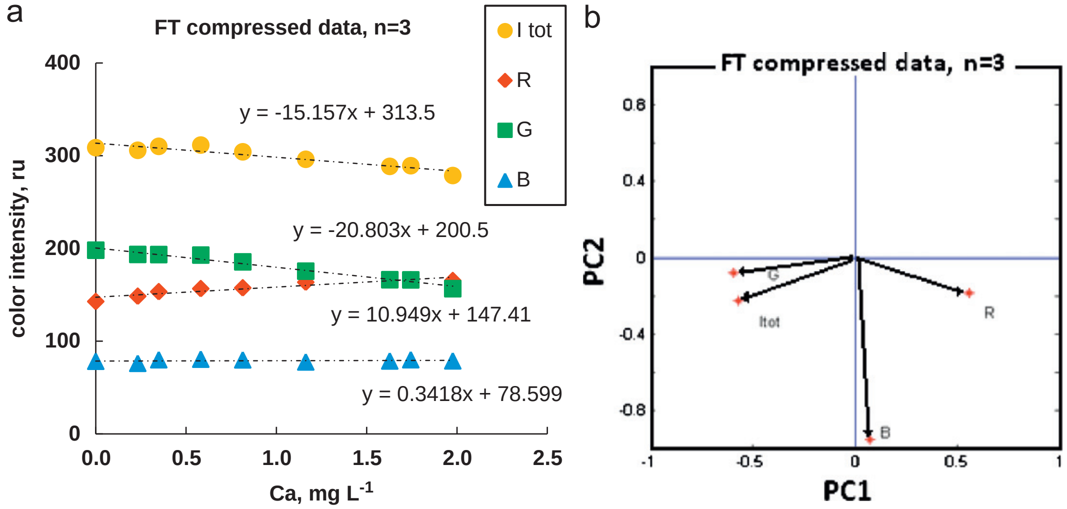

**Fig. 4.** Digital RGB data after compression by FT3, for orange solutions obtained in the standard calibration graph of Fig. 1. (a) Linear calibration using compressed color data; (b) Loading plots of color variables over PC1 and PC2. (For interpretation of the references to color in this figure legend, the reader is referred to the web version of this article.)

for the best range 0.2–2.0 mg $L^{-1}$of Ca(II), equation: $Y = -23.721\,X + 143.71$, ($R = 0.9977$).

The method exhibits a precision of 5.5%, relative standard deviation, rsd, for 1.0 mg $L^{-1}$ Ca(II).

The instrumental detection limit (3 $s_B$ criterion), $s_B$ being the standard deviation of the blank, was 0.07 mg $L^{-1}$.

The quality of the regression was verified by the statistical study of residuals and ANOVA. They confirmed the homoscedastic distribution of residuals and a significant linear regression.

Linear relationships between Ca(II) and other color variables deduced from the G basic color, such as log (G), G/R, or G/Itot ratios, were also studied as a means to maximize the precision. In all cases, results were not better than using only G.

Furthermore multivariate linear regression by Principal Component (PCR) was also deduced using the significant PC1. It was demonstrated that PC1 accounted for 89% of the initial variance and consequently the PCR included only PC1. The calibration responded to $C_{Ca} = 0.371$ PC1+0.943, $r = 0.98$. It transforms, to initial coordinates, as $C_{Ca,\ ppm} = 5.29 + 0.0159$ R − 0.0232–0.0051G–0.0124Itot. In this case, it was verified that a better calibration could be obtained by reduction of the calibration interval, up to 0.7 mg $L^{-1}$Ca. Consequently the use of PCR shortened the linear calibration range.

Also, other different chromatic-based parameters which have been proposed in the bibliography were studied as the calibration variable. So the parameters CPe, CPa, and CPl, as previously defined in the experimental section, were essayed. Also, the previous calibration by PCR (as inverse calibration, and taking into account PC1) was included.

The characteristics of the different regressions are gathered in Table 4. It allowed to evaluate and compare their analytical performance. It could be seen that calibrations by CPa and G presented the highest analytical sensitivity and maintained the maximum linear range. These two calibrations showed advantages and disadvantages. CPa exhibited higher sensitivity but also higher standard deviation of residuals than G. Consequently it could be said that, with CPa, the uncertainty would be widened.

Calibration by CPe and CPl exhibited a significant disadvantage: reduction of the linear range. The profile of CPl presented a typical sigmoid curve. A linear range could be obtained after reduction of the concentration interval. CPe was characterized by high values and required a transformation by log treatment.

**Table 4**
Ca content of different water samples analyzed by F-AAS and titrimetric method, as reference methods, and by the new colorimetric method with principal calibrations.

| Water sample | Ca(mg l$^{-1}$)[a] | | | | | |
|---|---|---|---|---|---|---|
| | **F-AAS method** | | **Complexometric titration** | **Digital image colorimetry-DIC** | | |
| | **Content** | **% Recovery, spiked samples** | **Content** | **Linear regression** | | **ANN-bp Calibration** |
| | | | | **G** | **CPa** | ***RGB*** |
| City net | 120.14 ± 2.47 | 103.3 | 174.19 ± 0.52 | 132.63 ± 3.43 | 142.15 ± 5.183 | 141.76 ± 1.08 |
| Mineral bottled | 41.36 ± 2.75 | 98.6 | 64.07 ± 0.26 | 41.74 ± 2.59 | 45.02 ± 3.76 | 40.65 ± 1.37 |
| Pyrenees' river | 52.90 ± 2.85 | 101.2 | 66.07 ± 0.26 | 53.18 ± 2.39 | 47.44 ± 4.95 | 59.43 ± 1.64 |

[a] Results are the average of three replicates ± standard deviation.

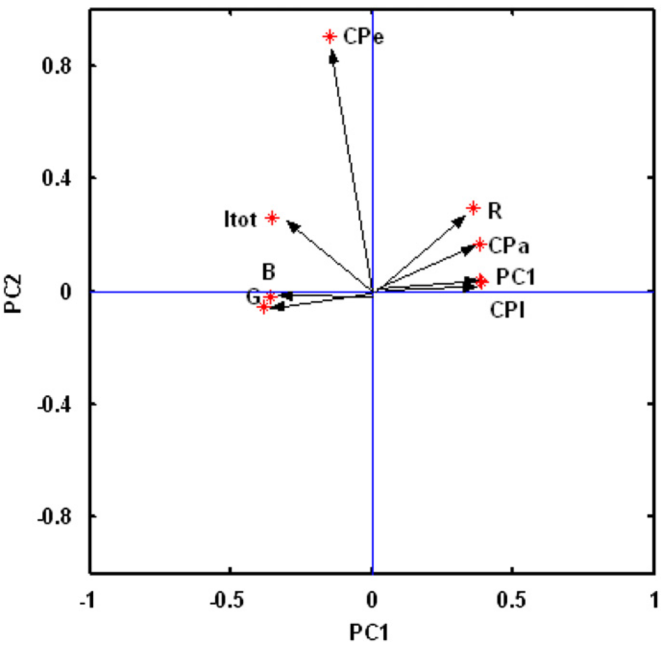

**Fig. 5.** Loading plot of the different chromatic parameters used as dependent variable in calibration graphs. (For interpretation of the references to color in this figure legend, the reader is referred to the web version of this article.)

In other words, the significance of the different chromatic variables was studied by PCA. That is, the calibration experience was evaluated taking into account the different chromatic variables R, G, B, $I_{tot}$,CPe, CPa, CPl and PC1.

The variance of the chromatic variables, after column-centering (in this case the variables showed high differences in magnitude), demonstrated that individual color, R G B, and CPa presented similar and high variance; however, the rest of the chromatic variables, except CPe, showed lower values.

The loading plot, for the different variables on PC1–PC2 gathered in Fig. 5, indicated that the chromatic parameters, CPa, CPl and PC1, were aligned toward R. Consequently their information showed a similarity and could be justifiable by the intrinsic significance of the R color. The CPe chromatic parameter was characterized by high values and tends to be associated with $I_{tot}$.

It could be argued that, in terms of analytical information, the most relevant chromatic parameters were G and CPa. They showed high analytical variance and sensitivity. The former was simpler and readily obtained while the latter retained a global chromatic information but with higher uncertainty.

### 3.6. *Neural network calibration*

Artificial Neural Network with back propagation of errors learning algorithm, ANN-bp [32], could be considered as a useful approach to model complex systems. It has a high generalization capacity with a minimum of experimental work. Consequently, it deserves to be explored in order to determine its performance in this field.

Neural study comprised the tuning of the architecture, net parameters and input variables.

Architectures studied consisted of three layers: input, hidden and output layers. However, best results were found with only two layers (only input–output). Those using more than three layers (one, and more than one, hidden layer) made the model less robust and augmented unnecessarily the time and the prediction error.

The number of input variables, input neurons, was demonstrated to be important. Training with only G color increased the training time. However, with four and, better, three color RGB, the training was fast, and results in the prediction step were reproducible. Output neuron answer was always maintained to one neuron.

Different transfer functions were studied: non-linear such as hyperbolic tangent sigmoid and log sigmoid, and also linear transfer functions. These last functions were always the best option. It offered fast training speed and reduced the mean squared error of the net. With regard to the training function, fast convergence was obtained by using the batch steepest descent training function.

Biases and weights were initialized randomly in the range [−1,1]. Data pretreatment was applied. Normalization was demonstrated to be efficient for fast convergence and better prediction.

This study showed the capability and opportunity of the neural net to make generalized predictions of Ca concentration. Notwithstanding, it also evidenced certain differences depending on the supplied information; best predictions could be attained by including the three basic colors while predictions based on only the G color were slower and with higher discrepancies.

The best neural predictions for the analysis of different types of water samples, using RGB data, are gathered in Table 4. These results showed high coincidence with those obtained by linear calibration.

### 3.7. *Application*

Calcium in different types of water and provenances, such as net of the city (Zaragoza, Spain), mineral bottled (trade mark) and Pyrenees river (Aragon river, Villanua, Huesca, Spain), was determined using the basic colorimetric data with previously discussed calibration methods. Samples were also analyzed by reference methods of FAAS, working at robust conditions and by complexometric reference titration using EDTA and EBT as indicator. In this last procedure, titrations were carried out at pH 10 with $NH_4Cl$–$NH_3$ buffer, to determine the total water hardness. The significant results are gathered in Table 4.

Reference method by FAAS could be compared with the standard procedure of water hardness determination, by complexometry. The results showed a high correlation and discrepancies were congruent with the analyte determined: only Ca by FAAS and total hardness, Ca and Mg mostly, by the titration method. The Ca content represented 80% of total hardness in the water of Pyrenees river while it ranged from 65% to 69% for the bottled and the city net water, respectively.

Recovery tests by FAAS were satisfactory, at levels of total recovery, and demonstrated the selectivity of the determination in all samples.

Comparison between reference values, by FAAS, with the best results by DIC always showed high coincidence. The lowest differences were always obtained by using the G color as dependent variable and with linear calibration, while CPa and RGB-ANN produced higher discrepancies. With G color, the differences were lower than 1% for the less concentrated samples of mineral and river waters. In the worst case, they were lower than 10%. The tendency of these differences showed that they were more important for samples with high concentration and could be justified in basis to the uncertainty that the sample conditioning (dilution), of concentrated samples, introduced in the results.

The statistical comparison by *t*-test of paired samples, between results by FAAS and the rest of the results by DIC, demonstrated that the *t*-critical value, at 95% confidence level, was 4.3, while the *t*-experimental values were /1.1/,/0.8/ and/ 1.3/ for the methods based on the G color, the CPa variable and the RGB-ANN method, respectively. That is, they were all lower than the *t*-critical value. Consequently, it could be said that the differences between the FAAS reference method and the new DIC determinations, despite the different calibrations, were not statistically significant. Discrepancies could be attributed to the normal distribution of results and there was confidence (95%) that the new method was not associated to any systematic error.

Studies on the application of the new colorimetric method as a ready-to-use method and field method were carried out. They allowed to evaluate its practicability as a fast method and in order to be practiced 'in situ'. So, different samples of water, of the Aragon River, were analyzed with simple equipment based on calibrated test tubes. They were used like sample cells to support the procedure. Images of samples were captured next to a calibration experience. Results were derived both after simple visual interpolation in the calibration or naked eye and also by fast measurement of the G basic color. Afterwards they were compared with analysis by FAAS in the laboratory. Observed discrepancies could be justified in basis to the quality of the calibration experience and also to the dilution steps in the sample conditioning. In any case the time of analysis could be reduced to the interval of minutes, calibration step included.

## 4. Conclusions

This paper is centered on digital image based methods with two main objectives: first, evaluation of the representativeness of the individual basic RGB colors and second, the application of this current technology to implement fast and reliable analytical methods.

Basic studies of the digital image colorimetry demonstrated the meaning of RGB data for analytical quantitative determinations. In the colorimeter model used, the existence of two significant participations was demonstrated: an intrinsic participation linked to the R color and a variable influence due to the G color. The latter showed the greatest variance of the system and the highest analytical sensitivity. Other chromatic parameters could be derived from individual basic colors, but there is no significant benefit over the measurements based on only one color.

The procedure could be implemented to provide calcium water hardness as a fast method based on capturing digital images with a photographic camera and only measuring the basic G color. The use of linear calibrations simplified the method and rendered a reasonable accuracy and precision. It demonstrated a great potential for high throughput analysis and could be applied as a field method with a capacity to perform water surveillance programs at low cost.

This study is part of a line based on the analytical application of digital image colorimetry and other analytes are currently being considered.

## Acknowledgment

The authors are thankful for the financial support by OX-CTA company (Huesca, Spain).

## Appendix A. Supporting information

Supplementary data associated with this article can be found in the online version at http://dx.doi.org/10.1016/j.talanta.2012.10.0387.

## References

[1] World Health Organization, J. Cotruvo, J. Bartram (Eds), Calcium and magnesium in drinking-water: public health significance, Geneva, 2009.
[2] WHO, Guidelines for Drinking-water quality, 4th edition, Geneva, 2011.
[3] International Standard, ISO 6058:1984, Water quality—Determination of calcium content—EDTA titrimetric method, Geneva,1984.
[4] B. Weltz, M. Sperling, Flame Atomic Absorption Spectrometry, Wiley-VCH, Weinheim, 2005.
[5] A. Montaser, D.W. Golightly, Inductively Coupled Plasmas in Analytical Atomic Spectrometry, 2nd Edition, VCH, Weinheim, Germany, 1992.
[6] S. Impedovo, A. Traini, P. Papoff, Talanta 18 (1971) 97.
[7] O. Hernandez, F. Jimenez, A.I. Jimenez, J.J. Arias, J. Have, Anal. Chim. Acta 320 (1996) 177.
[8] R.A.Z. Lima, S.R.B. Santos, R.S. Costa, G.P.S. Marcone, R.S. Honorato, V.B. Nascimento, M.C.U. Araujo, Anal. Chim. Acta 518 (2004) 25.
[9] G.Z. Tsogas, D.L. Giokas, A.G. Vlessidis, Talanta 80 (2010) 2049.
[10] K. Vahl, H. Kahlert, F. Scholz, Electroanalysis 22 (2010) 2172.
[11] T.M. Lerga, C.K. O'Sullivan, Anal. Chim. Acta 610 (2008) 105.
[12] M.U. Heumann, Fresenius J. Anal. Chem. 354 (1996) 803.
[13] International Standard, ISO 17381:2003, Water quality—Selection and application of ready-to-use test kit methods in water analysis, Geneva, 2003.
[14] L. Byrne, J. Barker, G.P. Thomas, D. Diamond, Trends Anal. Chem. 19 (2000) 517.
[15] A. Lopez-Molinero, D. Liñan, D. Sipiera, R. Falcon, Microchem. J. 96 (2010) 380.
[16] A.R. Torres, W.S. Lyra, S.I. Evangelista, R.A.N. Andrade, E.C. da Silva, M.C.U. Araujo, E.N. Gaiao, Talanta 84 (2011) 601.
[17] K. Tohda, M. Gratzl, Anal. Sci. 22 (2006) 937.
[18] A.W. Martinez, S.T. Phillips, E. Carrilho, S.W. Thomas, H. Sindi, G.M. Whitesides, Anal. Chem. 80 (2008) 3699.
[19] M. Kompany-Zareh, S. Mirzaei, Anal. Chim. Acta 521 (2004) 231.
[20] Y. Suzuki, M. Endo, J. Jin, K. Iwase, M. Iwatsuki, Anal. Sci. 22 (2006) 411.
[21] M. Vidal, J.M. Amigo, R. Brob, F. van den Bergb, M. Ostra, C. Ubide, Anal. Chim. Acta 706 (2011) 1.
[22] A. Choodum, N. NicDaeid, Talanta 86 (2011) 284.
[23] A. Choodum, N. NicDaeid, Drug Test Anal. 3 (2011) 277.
[24] L. Lahuerta Zamora, P. Alemán López, G.M. Antón Fosa, R. Martín Algarrac, A.M. Mellado Romero, J. Martínez Calatayud, Talanta 83 (2011) 1575.

[25] C. Zhang, K.S. Suslick, J. Am. Chem. Soc. 127 (2005) 11548.

[26] A. Lapresta-Fernandez, L.F. Capitan-Vallvey, Analyst 136 (2011) 3917.

[27] A. Lapresta-Fernández, L.F. Capitán-Vallvey, Anal. Chim. Acta 706 (2011) 328.

[28] W.S. Lyra, V.B. dos Santos, A.G.G. Dionizio, V.L. Martins, L.F. Almeida, E.N. Gaiao, P.H. Gonzalves, E.C. da Silva, M.C.U. Araujo, Talanta 77 (2009) 1584.

[29] W.S. Lyra, F.A.C. Sanches, F.A.S. Cunha, P.H. Gonzalves, S. Guimaraes, E.C. da Silva, M.C.U. Araujo, Anal. Methods 3 (2011) 1975.

[30] E.N. Gaiao, V.L. Martins, W.S. Lyra, L.F. de Almeida, E.C. da Silva, M.C.U. Araujo, Anal. Chim. Acta 570 (2006) 283.

[31] Z. Marczenko, Separation and Spectrophotometric Determination of Elements, Ellis Horwood Ltd, New York, 1986.

[32] J. Zupan, J. Gasteiger, Neural Networks for Chemists, VCH, Weinheim, 1993.